

Synthesis of Manganese Tetroxide Nanoparticles Using Precipitation and Study of Its Structure and Optical Characteristics

Reza Shokoohi,¹ Mohammad Taghi Samadi,¹ Ghorban Asgari,² Mohammad Vanaei Tabar,^{1,*} and Kazem

Godini¹

¹Department of Environmental Health Engineering, Faculty of Health and Research Center for Health Sciences, Hamadan University of Medical Sciences, Hamadan, IR Iran

²Social Determinants of Health Research Center (SDHRC), Department of Environmental Health Engineering, School of Public Health, Hamadan University of Medical Sciences, Hamadan, IR Iran

*Corresponding author: Mohammad Vanaei Tabar, Department of Environmental Health Engineering, Faculty of Health and Research Center for Health Sciences, Hamadan University of Medical Sciences, Hamadan, IR Iran. E-mail: m.vanaei367@gmail.com

Received 2016 August 29; Revised 2016 November 21; Accepted 2016 December 21.

Abstract

Considering extensive applications of manganese tetroxide nanoparticles in various industries due to its special properties, conducting studies on how to achieve more suitable ways to produce smaller nanoparticles is of great importance. In this study, nanoparticles of manganese tetroxide (Mn_3O_4) were synthesized by a co-precipitation method. In order to determine the characteristics of the structure, size, and specific surface of the resulting nanoparticles, techniques such as XRD, BET, BJH, FESEM, and FTIR were employed. Also, the nanoparticles were quantified with EDS and their colony size was examined using DLS experiments. The findings revealed a production of crystalline manganese tetroxide nanoparticles with a space group of $141/amd$ (S.G.) (141) and a molecular weight of 228.81 with the international code of ICSD Card # 89 - 4837. The specific surface area was $32.147 \text{ m}^2/\text{g}$ with a pore volume of $0.1041 \text{ cm}^3/\text{g}$. The XRD and EDX analyses verify the production of the Mn_3O_4 nanoparticles. The size of the nanostructures is approximately 19 nm. The method used in this study could produce the Mn_3O_4 nanoparticles in a much easier way without the need for surfactants. Compared to the nanoparticles produced in other studies, the size of the nanoparticles produced in the present study is remarkably smaller. Moreover, less amount of the metal salt was used.

Keywords: Mn_3O_4 Nanoparticles Synthesis, Co-Precipitation, Structural Characteristics

1. Introduction

Nano is one of the most modern technologies and has been used in various fields, especially for the removal of various pollutants from wastewater, because of its high potentiality and unique characteristics (1). Co-precipitation is considered as one of the main and first chemical methods for making nanoparticles. In this method, a dissolved substance is changed to an insoluble one (2). In general, the composition of poorly soluble products from the aqueous phase forms the base of this method (3). The base of wet chemical methods for the synthesis of nanoparticles consists of many rudimentary chemical reactions (4). Manganese oxides are crystallized into 4 modes: MnO , Mn_3O_4 , Mn_2O_3 , and Mn_2O according to the 4 forms of oxidation (5). These composites are used in wastewater treatment, catalysis, sensors, super-capacitors, and alkaline and rechargeable batteries. Mn_3O_4 , as an important functional oxide, shows some magnetic, ion exchange, electrochemical, and catalytic properties (6). These properties give the compound the potential for being applied in many operations such as use as a catalyst (2), an electrode (7), and as a magnetic tool (8). Of all the synthesis methods and structure

control in producing Mn_3O_4 nanostructures, one can, for example, refer to co-precipitation (9), thermal decomposition (10), the process of molding (11), and sol-gel (12). Many water-soluble catalysts may be harmful to the environment; this is not the case for the Mn_3O_4 compounds since these can be recycled due to the same structure (13). Mn_3O_4 is an environmentally friendly compound. It can even be more effective in removing organic compounds than iron nanoparticles. For instance, Mn_3O_4 is one of the most common catalysts for the oxidation of CH_4 and carbon, and it acts selectively in the removal of nitrobenzene. The destruction of nitrogen oxides and oxide hydrogenation of alcohol is another application of Mn_3O_4 . This compound is used in the magnetic industry for the production of soft magnetic materials and in the electrochemical industry as a raw material for the production of electrodes for Li-Mn-O in the production of lithium batteries (14). In this study, a new, easy, and low-cost measure was utilized for producing hydrophilic nanoparticles of Mn_3O_4 .

2. Methods

2.1. Materials and Apparatus

Potassium permanganate (KMnO_4) (+99%) and hydrazine monohydrate ($\text{N}_2\text{H}_4 \cdot \text{H}_2\text{O}$) (98%) were purchased from MERCK (Germany). Other required materials during the tests such as ethanol, sulfuric acid, and sodium hydroxide were also bought from the same company and used for the experiments with no change.

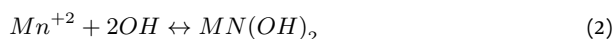
2.2. Synthesis of Mn_3O_4 Nanoparticles

The present study was conducted in a pilot-scale in both laboratory water and wastewater at the school of public health at the Hamadan University of Medical Sciences.

A 4 mmol sample of KMnO_4 was well dissolved in 200 mL of distilled water on a magnetic mixer at an ambient temperature (22°C). Two hundred ml of the $\text{N}_2\text{H}_4 \cdot \text{H}_2\text{O}$ solution containing 40 mmol of $\text{N}_2\text{H}_4 \cdot \text{H}_2\text{O}$ was quickly added to it on the high-speed mode of the mixer. Under such conditions, the color of the solution altered from purple to dark brown.

The pH of the resulting solution was fixed at 9 with 1 M H_2SO_4 while quick mixing. Then, the solution was slowly mixed at 70°C for 15 minutes by means of a mixer. Over time, while forming the structure of the nanoparticles, the color of the solution transformed from dark brown to brown-orange and the formed particles appeared clearly as colonies after 15 minutes. At this stage, the solution was cooled down to reach room temperature and the settled particles were separated through centrifugation. The resulting particles were then rinsed twice with distilled water and once with ethanol; next, they were dried out for 8 hours in an oven at 50°C . To demonstrate the structural properties of the nanoparticles, the X-ray diffraction (XRD) was used at room temperature by means of a D8 Advance diffractometer (Bruker, Germany) method. The angle of 2θ was considered between 5 and 90 degrees in this analysis. The source of light scattering was ($\lambda = 1.540589 \text{ \AA}$) Cu. The results were evaluated with Xpert software. Moreover, the size and specific surface of this compound was examined by using the BET and Barrett-Joyner-Halenda (BJH) methods. Further, in order to display the image of the produced nanoparticles, the FESEM device was used. Finally, the magnetic spectrum of the nanoparticles was examined with the Fourier transform infrared (FTIR) method (14).

Reactions happening in this process were as follows (3):



These reactions 1 - 4 occurred under lab conditions. Time and temperature only have an influence on the size and specific surface of the nanoparticle. In this study, temperature and time were set to 70°C and 15 minutes, respectively (15).

3. Results and Discussion

3.1. Analysis of BET and BJH

In order to measure the surface area of Mn_3O_4 nanoparticles, the Brauner-Emmett-Taylor (BET) method was utilized with a partial pressure of 0.25 to 0.02, based on nitrogen absorption (16).

The following formula was used to estimate the size of the nanoparticles:

$$D = \frac{6}{\rho \times S_{BET}} \quad (5)$$

Where, ρ represents the density of the nanoparticles, which for nanoparticles Mn_3O_4 is equal to 4.876 g/cm^3 . The mentioned equation is applicable for spherical particles; assuming a spherical structure of Mn_3O_4 nanoparticles. The results show that nanoparticles are produced with a size of 19.479 nm. It was found that the specific surface area was $32.147 \text{ m}^2/\text{g}$. Table 1 displays a breakdown of the results.

Table 1. Results of the BET Analysis for Mn_3O_4 Nanoparticles

Title	Unit	Amount
Sample amount	g	0.3
Pressure in experimental conditions	KPa	86.832
Average size of nanoparticles	nm	19.479
ASBET	m^2/g	32.45
ρ/ρ_0 (relative pressure)	-	0.983

Adsorption and desorption charts for Mn_3O_4 nanoparticles are presented in Figure 1.

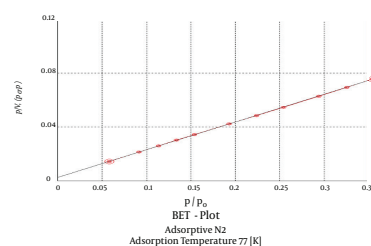


Figure 1. Adsorption and Desorption for Mn_3O_4 Nanoparticles

The BJH test was also done to determine the porosity of the nanoparticles (Table 2). The total volume of the pores was found to be 0.1041 cm³/g. According to the formula $d = 4V/A$, the pore size and surface area are related, where V is the total volume of the pores that can be calculated from adsorption and desorption and A is the specific surface area (BET).

Table 2. Results of BJH Analysis for Mn₃O₄ Nanoparticles

Title	Unit	Amount
Sample amount	g	0.3
Pressure in experimental conditions	KPa	86.832
Average size of nanoparticles	nm	19.479
ASBET	m ² /g	32.45
ρ/ρ_0 (relative pressure)	-	0.983
Pore radius (rp)	nm	3.09

In order to calculate the pore radius, the Kelvin equation was used as follows:

$$r_k (A) = \frac{4.15}{\log \frac{P}{P_0}} \quad (6)$$

$$r_\rho = r_k + t \quad (7)$$

Where, rp is the actual pore radius, rk is the Kelvin radius in Angstrom, and t is the thickness of the adsorbed layer.

In recent years, several studies have been conducted to produce nanoparticles of Mn₃O₄. Our method is efficiently capable of competing with other methods and also has advantages in comparison to these methods. Among these advantages, one can refer to the short time process, the lack of environmental pollutants such as surfactants, production at atmospheric pressure and thus easier navigation, and producing smaller particles in small sizes.

In order to compare the studied method with other methods, some examples of other methods are described below.

In the solvothermal method, autoclave is used to control the temperature and pressure. The time required to complete the production process is between 8 and 24 hours and temperature should be fixed at approximately 160°C. In this way, the nanoparticles have an average size of 135 nm, which is several times larger than by using the chemical deposition method (17).

In the hydrothermal method, the time needed is about 24 hours. The operation of this method is more difficult because the temperature and pressure must be fully controlled since its pressure and ambient temperature is not

operative and the size of the produced particles is between 300 and 500 nm this way (18).

The chemical deposition method is the same as other methods, except that in other studies surfactants are used, which after washing nanoparticles produce concentrated wastewater that contains surfactant. In this study, we tried to address this problem. Moreover, in a study conducted by Vijayalakshmi and Pauline the size of the nanoparticles produced by this method was approximately 500 nm (19).

3.2. Analysis of FESEM and EDS

In this study, in order to examine the morphology and shape of the Mn₃O₄ nanoparticles, the FESEM device was applied with a magnification of 7,000,000 times. Figure 2 displays this image. The device is equipped with advanced EDS, which is useful for the FESEMI-quantitative analysis of elements as well as for linear and volumetric analyses (20). As can be seen in Figure 2, the shape of the nanoparticles is spherical and has a diameter of between 8 and 23 nm. Figure 3 shows an image of the produced nanoparticles.

The results of the EDS test have been presented in Figure 4. This analysis is implemented for the quantitative study of the production of small samples and the verification of the results of other tests used in this study (Table 3).

3.3. Analysis of XRD

In order to examine and characterize the obtained structure, the X-ray diffraction (XRD) method was used. Figure 5 displays the pattern of XRD as an example. As can be seen, the obtained peaks correspond to the compound of Hausmannite tetragonal manganese tetroxide with the space group of (141) I41/amd (S.G.) and the molar weight of 228.81. Also, it has the international code of ICSD Card # 89-4837. Moreover, the space network data sample was determined as follows: $a = 5.763 \text{ \AA}$, $C = 9.456 \text{ \AA}$ and $V = 314.0 \text{ \AA}^3$. It should be noted that in this analysis, no other composition with a substantial amount was detected, illustrating the purity of the sample.

According to the results obtained from the analysis of the nanoparticles by the software, the tallest peak of the graph displays Mn₃O₄ nanoparticles with a size of 23 nm. In order to determine the size this way, the Scherrer equation was used, which shows the connection between the size and width of the peaks (21). The supposed equation is as follows (22):

$$B = \frac{k\lambda}{L \cos \theta} \quad (8)$$

Where, B presents the width of the peak (full width at half maximum), λ is the wavelength of X-ray, L is the size of

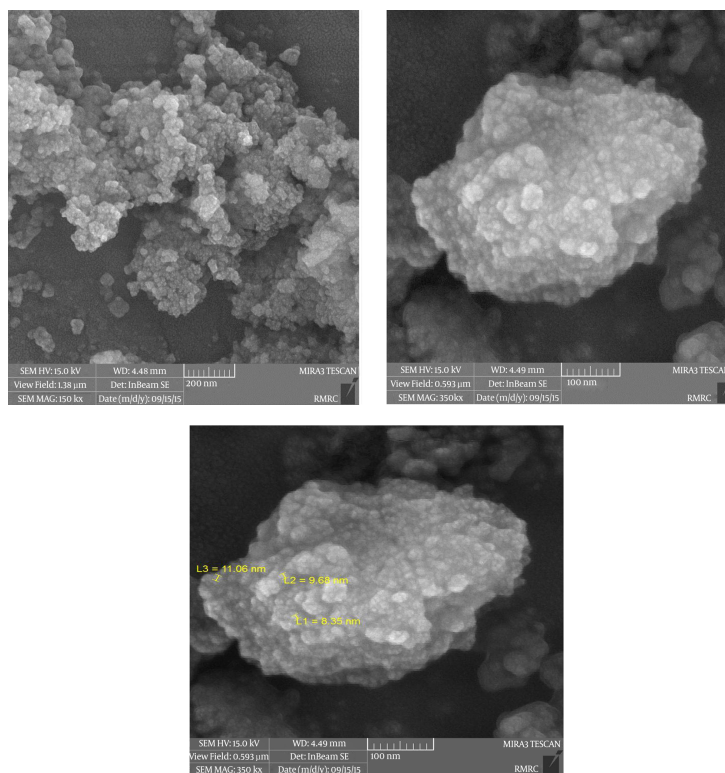


Figure 2. FESEM Images of the Nanoparticles for Mn_3O_4

Table 3. Obtained Results of the EDS Analysis for Mn_3O_4 Nanoparticles

Elt	Line	Int	Error	K	Kr	W%	A%	ZAF	Formula	Ox%	Pk/Bg	Class	LConf	HConf	Cat#
O	Ka	29.3	0.4517	0.0723	0.0640	12.80	31.64	0.5000		0.00	10.59	A	12.06	13.54	0.00
S	Ka	52.5	0.9458	0.0608	0.0538	5.84	7.21	0.9209		0.00	7.96	A	5.59	6.10	0.00
K	Ka	63.8	0.6005	0.0996	0.0882	8.80	8.90	1.0020		0.00	9.52	A	8.46	9.15	0.00
Mn	Ka	217.0	0.7975	0.7674	0.6796	72.56	52.25	0.9367		0.00	39.18	A	71.02	74.10	0.00



Figure 3. Image of Mn_3O_4 Nanoparticles

the particle, θ is the angle between radiation ray and screen (particle) and K represents the constant.

The width of the sample provides information about the sample. Crista field size and micro-strain (short-range strain that is caused by lattice defects) are among the factors affecting the bandwidth of the peaks. It is obvious that the larger the crystal lattice defects with less imperfections (21), the less wide the peaks will be (22). In this study, the obtained pattern from X-ray diffraction corresponds to similar studies conducted to produce Mn_3O_4 nanoparticles (17), which confirms the results obtained in this study (19).

3.4. FTIR Analysis

Figure 6 shows the FTIR spectrum for Mn_3O_4 nanoparticles. As can be seen, this sample shows several peaks in

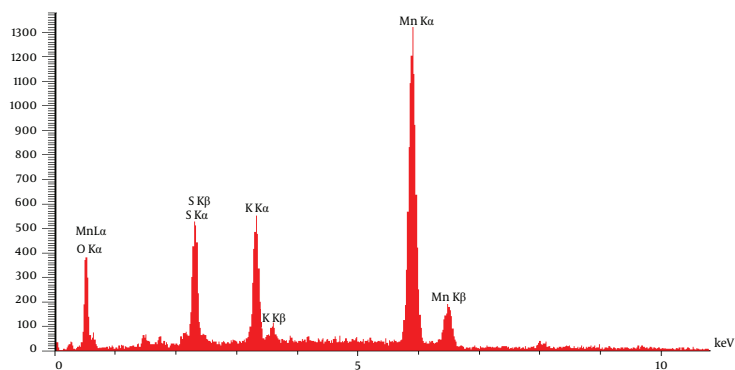


Figure 4. EDS sample for Mn₃O₄ Nanoparticles

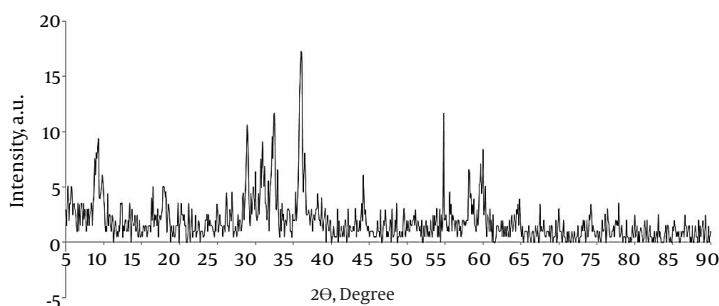


Figure 5. X-ray Diffraction Pattern for Mn₃O₄ Nanoparticles

the range of 1000 - 1637, as well as in the range of 400-1000, and two peaks in the range of 3324 - 3436.

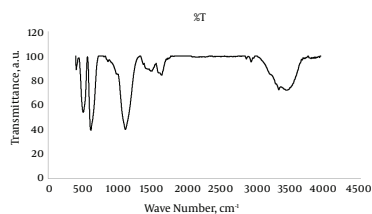


Figure 6. FTIR Spectrum for Mn₃O₄ Nanoparticles

Absorption peaks in the range of 400 - 1000 indicate the presence of the octahydrals of MnOx in the sample (5). Also, the presence of peaks in the range of 1637 - 1000 defines the vibrational bands of O-H attached to the manganese atoms (14). Also, the peaks in the area of 3324 and 3436 introduce the NH band on hydrazine monohydrate with the molecular formula of N₂H₄. The results of this analysis are consistent with the results obtained in previous studies in which functional groups were evaluated in the production of nanoparticles of Mn₃O₄ (23).

The studies conducted on the samples showed that the formula $\alpha = 2.33A/t$ is used for the determination of the absorption coefficient. And, in order to determine the optical gap for Mn₃O₄ nanoparticles, the equation $\alpha h\nu = k(h\nu - \epsilon)^{1/2}$ is used (24).

In this formula, h represents the photon energy, k is the constant and ϵ stands for the optical gap. Thus, the optical gap for a thin layer of Mn₃O₄ nanoparticles has been reported as 2 eV. It should be noted that the energy gap for the optical thin layer of these nanoparticles was estimated at 2 eV. Figure 7 below displays the linear fit graph of the results.

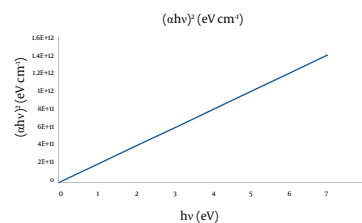


Figure 7. Linear Fit Graph of the Mn₃O₄ Nanoparticles

3.5. Analysis of DLS

Dynamic light scattering (DLS) is a useful technique for measuring the size of nanoparticles and determining their characterization in the samples of the solution (25). In this method, the laser light is shone on the sample containing the colloid and after passing through the sample, the intensity of scattered light is measured, which is related to the mechanical size of nanoparticles. The larger particles scatter less light and smaller particles scatter more light (26).

As the particles form colonies during manufacturing and drying, we used this method for measuring the size of the nanoparticle colonies (26). The results have been presented in Figure 8 and show the size of the colonies at about 100 to 150 nm. It should be noted that this analysis has not been reported on Mn₃O₄ nanoparticles to date.

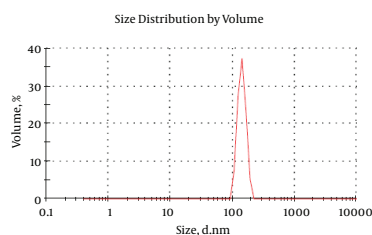


Figure 8. DLS Pattern for Mn₃O₄ Nanoparticles

In the method of solvothermal synthesis, in order to control temperature and pressure, an autoclave is used because the process requires 8 - 24 hours to be completed and temperature should be set at 160°C. In the study by Zhang et al. who investigated this method for the production of manganese tetroxide nanoparticles, it was found that the average size of the produced nanoparticles was 135 nm, which is several times larger than the co-precipitation (17). The hydrothermal method is also used for production of manganese tetroxide nanoparticles; in this method, 24 hours are needed for completion and its operation requires more effort since both temperature and pressure must be completely controlled. Furthermore, the investigation of Ashoka et al. claimed that the size of the produced nanoparticles was approximately between 300 and 500 nm (18). The main disadvantage of the chemical co-precipitation is generation of wastewater containing surfactant. In this study, we aimed to solve this problem. More importantly, the size of the produced nanoparticles was larger in comparison with the results of other studies such as the size of 500 nm reported by Vijayalakshmi and Pauline (19).

4. Conclusions

The method used in this study could produce Mn₃O₄ nanoparticles. To determine the degree of crystallization and other specifications, different analyses were performed on the Mn₃O₄ nanoparticles including: XRD, BET and BJH, FESEM, measuring FTIR range, quantitative measurement of Mn₃O₄ nanoparticles using EDS, and measuring the colony of particles through DLS. According to the conducted analyses, the produced particles have a high purity. In this way, in addition to ease of implementation, the consumable materials have been used in the best way so that high production efficiency is achieved and advantage is taken from using the metal salt. Based on the results, the size of the nanoparticles is also based on nanometers.

Acknowledgments

This article is part of a thesis entitled "Evaluation of the efficiency of hybrid processes of nanoparticles of manganese tetroxide/hydrogen peroxide (Mn₃O₄/H₂O₂) and Mn₃O₄/proxy Monosulfat (Mn₃O₄/H₃K₅O₁₈S₄) to remove polyvinyl alcohol from aqueous environments." This thesis was approved by the vice chancellor for research and technology of Hamadan University of Medical Sciences in 2015, which was conducted with the support of this department.

References

1. Teja AS, Koh P. Synthesis, properties, and applications of magnetic iron oxide nanoparticles. *Prog Crystal Growth Character Mat.* 2009;**55**(1-2):22-45. doi: [10.1016/j.pcrysgrow.2008.08.003](https://doi.org/10.1016/j.pcrysgrow.2008.08.003).
2. Cui H, Feng Y, Ren W, Zeng T, Lv H, Pan Y. Strategies of large scale synthesis of monodisperse nanoparticles. *Recent Pat Nanotechnol.* 2009;**3**(1):32-41. [PubMed: [19149753](https://pubmed.ncbi.nlm.nih.gov/19149753/)].
3. Cushing BL, Kolesnichenko VL, O'Connor CJ. Recent advances in the liquid-phase syntheses of inorganic nanoparticles. *Chem Rev.* 2004;**104**(9):3893-946. doi: [10.1021/cr030027b](https://doi.org/10.1021/cr030027b). [PubMed: [15352782](https://pubmed.ncbi.nlm.nih.gov/15352782/)].
4. Riahi-Belkaoui A. *Accounting Theory*. Cengage Learning EMEA. International Thomson; 2004.
5. Moses Ezhil Raj A, Victoria SG, Jothy VB, Ravidhas C, Wollschlager J, Suendorf M, et al. XRD and XPS characterization of mixed valence Mn₃O₄ hausmannite thin films prepared by chemical spray pyrolysis technique. *Appl Surface Sci.* 2010;**256**(9):2920-6. doi: [10.1016/j.apsusc.2009.11.051](https://doi.org/10.1016/j.apsusc.2009.11.051).
6. Yamashita Y, Mukai K, Yoshinobu J, Lippmaa M, Kinoshita T, Kawasaki M. Chemical nature of nanostructures of La_{0.6}Sr_{0.4}MnO₃ on SrTiO₃(100). *Surface Sci.* 2002;**514**(1-3):54-9. doi: [10.1016/s0039-6028\(02\)01607-2](https://doi.org/10.1016/s0039-6028(02)01607-2).
7. Wang YG, Cheng L, Li F, Xiong HM, Xia YY. High Electrocatalytic Performance of Mn₃O₄/Mesoporous Carbon Composite for Oxygen Reduction in Alkaline Solutions. *Chem Mat.* 2007;**19**(8):2095-101. doi: [10.1021/cm062685t](https://doi.org/10.1021/cm062685t).
8. Salazar-Alvarez G, Sort J, Surinach S, Baro MD, Nogues J. Synthesis and size-dependent exchange bias in inverted core-shell MnO/Mn₃O₄ nanoparticles. *J Am Chem Soc.* 2007;**129**(29):9102-8. doi: [10.1021/ja0714282](https://doi.org/10.1021/ja0714282). [PubMed: [17595081](https://pubmed.ncbi.nlm.nih.gov/17595081/)].

9. Ahmad T, Ramanujachary KV, Lofland SE, Ganguli AK. Nanorods of manganese oxalate: a single source precursor to different manganese oxide nanoparticles (MnO, Mn₂O₃, Mn₃O₄). *J Mat Chem*. 2004;**14**(23):3406. doi: [10.1039/b409010a](https://doi.org/10.1039/b409010a).
10. Sun X, Zhang YW, Si R, Yan CH. Metal (Mn, Co, and Cu) oxide nanocrystals from simple formate precursors. *Small*. 2005;**1**(11):1081-6. doi: [10.1002/smll.200500119](https://doi.org/10.1002/smll.200500119). [PubMed: [17193400](https://pubmed.ncbi.nlm.nih.gov/17193400/)].
11. Jiao F, Harrison A, Hill AH, Bruce PG. Mesoporous Mn₂O₃ and Mn₃O₄ with Crystalline Walls. *Adv Mat*. 2007;**19**(22):4063-6. doi: [10.1002/adma.200700336](https://doi.org/10.1002/adma.200700336).
12. Lei S, Tang K, Fang Z, Zheng H. Ultrasonic-Assisted Synthesis of Colloidal Mn₃O₄ Nanoparticles at Normal Temperature and Pressure. *Crystal Growth Design*. 2006;**6**(8):1757-60. doi: [10.1021/cg050402o](https://doi.org/10.1021/cg050402o).
13. Cole-Hamilton DJ. Homogeneous catalysis—new approaches to catalyst separation, recovery, and recycling. *Science*. 2003;**299**(5613):1702-6. doi: [10.1126/science.1081881](https://doi.org/10.1126/science.1081881). [PubMed: [12637737](https://pubmed.ncbi.nlm.nih.gov/12637737/)].
14. Gibot P, Laffont L. Hydrophilic and hydrophobic nano-sized Mn₃O₄ particles. *J Solid State Chem*. 2007;**180**(2):695-701. doi: [10.1016/j.jssc.2006.11.024](https://doi.org/10.1016/j.jssc.2006.11.024).
15. Li X, Zhou L, Gao J, Miao H, Zhang H, Xu J. Synthesis of Mn₃O₄ nanoparticles and their catalytic applications in hydrocarbon oxidation. *Powder Technol*. 2009;**190**(3):324-6. doi: [10.1016/j.powtec.2008.08.010](https://doi.org/10.1016/j.powtec.2008.08.010).
16. Garrido J, Linares-Solano A, Martin-Martinez JM, Molina-Sabio M, Rodriguez-Reinoso F, Torregrosa R. Use of nitrogen vs. carbon dioxide in the characterization of activated carbons. *Langmuir*. 1987;**3**(1):76-81. doi: [10.1021/la00073a013](https://doi.org/10.1021/la00073a013).
17. Zhang W, Yang Z, Liu Y, Tang S, Han X, Chen M. Controlled synthesis of Mn₃O₄ nanocrystallites and MnOOH nanorods by a solvothermal method. *J Crystal Growth*. 2004;**263**(1-4):394-9. doi: [10.1016/j.jcrysgr.2003.11.099](https://doi.org/10.1016/j.jcrysgr.2003.11.099).
18. Ashoka S, Nagaraju G, Chandrappa GT. Reduction of KMnO₄ to Mn₃O₄ via hydrothermal process. *Mat Lett*. 2010;**64**(22):2538-40. doi: [10.1016/j.matlet.2010.08.003](https://doi.org/10.1016/j.matlet.2010.08.003).
19. Vijayalakshmi S, Pauline S. Synthesis, Structural and Morphological Characterization of CTAB-Mn₃O₄ by CO Precipitation Method. *Synthesis*. 2014;**6**(7):3813-1815.
20. Whyte IM, Buckley NA, Reith DM, Goodhew I, Seldon M, Dawson AH. Acetaminophen causes an increased International Normalized Ratio by reducing functional factor VII. *Ther Drug Monit*. 2000;**22**(6):742-8. [PubMed: [11128244](https://pubmed.ncbi.nlm.nih.gov/11128244/)].
21. Dorset DL. X-ray Diffraction: A Practical Approach. *Microsc Microanal*. 1998;**4**(5):513-5. doi: [10.1017/S143192769800049X](https://doi.org/10.1017/S143192769800049X). [PubMed: [18613987](https://pubmed.ncbi.nlm.nih.gov/18613987/)].
22. Singh AK. Advanced x-ray techniques in research and industry. IOS Press; 2005.
23. Shukla N, Liu C, Jones PM, Weller D. FTIR study of surfactant bonding to FePt nanoparticles. *J Magnet Magnet Mat*. 2003;**266**(1-2):178-84. doi: [10.1016/s0304-8853\(03\)00469-4](https://doi.org/10.1016/s0304-8853(03)00469-4).
24. Xu HY, Xu S, Wang H, Yan H. Characterization of Hausmannite Mn₃O₄ Thin Films by Chemical Bath Deposition. *J Electrochem Soc*. 2005;**152**(12):C803. doi: [10.1149/1.2098267](https://doi.org/10.1149/1.2098267).
25. Takahashi K, Kato H, Saito T, Matsuyama S, Kinugasa S. Precise Measurement of the Size of Nanoparticles by Dynamic Light Scattering with Uncertainty Analysis. *Particle Particle Systems Character*. 2008;**25**(1):31-8. doi: [10.1002/ppsc.200700015](https://doi.org/10.1002/ppsc.200700015).
26. Jans H, Liu X, Austin L, Maes G, Huo Q. Dynamic light scattering as a powerful tool for gold nanoparticle bioconjugation and biomolecular binding studies. *Anal Chem*. 2009;**81**(22):9425-32. doi: [10.1021/ac901822w](https://doi.org/10.1021/ac901822w). [PubMed: [19803497](https://pubmed.ncbi.nlm.nih.gov/19803497/)].